*GEOLOGICA CARPATHICA, 49, 1, BRATISLAVA, FEBRUARY 1998*
*15–32*

# THE NEOGENE REMAGNETIZATION AND PETROMAGNETIC STUDY OF THE EARLY CRETACEOUS LIMESTONE BEDS FROM THE RÍO ARGOS (CARAVACA, PROVINCE OF MURCIA, SE SPAIN)

PHILIP J. HOEDEMAEKER[1], MIROSLAV KRS[2], OTAKAR MAN[2], JOSEP M. PARÉS[3], PETR PRUNER[2] and DANIELA VENHODOVÁ[2]

[1]National Museum of Natural History, Postbus 9517, 2300 RA Leiden, Netherlands
[2]Geological Institute, Academy of Sciences of the Czech Republic, Rozvojová 135, 165 00 Prague 6 — Lysolaje, Czech Republic
[3]Institute of Earth Sciences, "Jaume Almera", Lluís Solé i Sabarís s/n, 08028 Barcelona, Spain

*(Manuscript received March 18, 1997; accepted in revised form December 11, 1997)*

**Abstract:** The Early Cretaceous limestone strata around the Río Argos (Caravaca Region, Province Murcia, SE Spain) were selected for magnetostratigraphic investigations. This section was chosen due to its importance, detailed geological and paleontological documentation and good outcrops of individual strata. Altogether 361 oriented hand samples were collected covering the Berriasian, Valanginian, Hauterivian, Barremian and the Early Aptian sequence strata. The laboratory specimens were subjected to both the alternating-field and thermal demagnetization procedures, while the thermal treatment by means of the MAVACS apparatus was carried out at relatively dense temperature steps up to 590 °C, in many cases up to 690 °C. Twenty pilot samples were tested for the anisotropy of magnetic susceptibility. Fifteen samples were selected for detailed analysis with the aim of determining the unblocking temperatures with higher precision and verifying the possible occurrence of self-reversal phenomena of remanence during laboratory thermal treatments. All the 361 collected samples were subjected to systematic thermal or combined demagnetization procedures. Multi-component analysis was applied to separation of respective remanent magnetization components, Fisher's (1953) statistics were used for the calculation of the separated remanence components combined with fold tests. — Few samples were found totally weathered, these are characterized by low unblocking temperatures (below 100 °C), and their magnetic susceptibility is markedly lower. The vast majority of samples showed three components of remanence, A-, B- and C-components. It was clearly proved that the studied un-weathered limestones can be divided into two groups of rocks, the first group with syn-tectonic magnetization, and the second group of limestones totally remagnetized in the Neogene. This way, the Early Cretaceous limestones from the Río Argos were found unsuitable for derivation of a magnetostratigraphic scale. Apart from totally weathered limestones, magnetite with a well defined unblocking temperature (around 540 °C) was found as the carrier of remanent magnetization in the majority of massive and fresh-looking limestone samples. From the study of the anisotropy of magnetic susceptibility it could be concluded that the fabric of the limestones in both the groups of totally and partially remagnetized samples showed the same features. It is of interest that the limestones under study display no signs of thermal, hydrothermal, chemical, dynamometamorphic or other alterations. The principal aim of the paper is to demonstrate typical case histories aimed at methodological problems since similar rocks may be selected for magnetostratigraphic studies in other regions of the Tethyan realm and similar remagnetization phenomena may be encountered as already described in the papers by Villalaín et al. (1996), Parés & Roca (1996).

**Key words:** SE Spain, Province Murcia, the Río Argos area, Early Cretaceous limestones, petromagnetism and magnetomineralogy, anisotropy of magnetic susceptibility, remagnetization.

## Introduction

The global pattern of normal and reverse magnetozones may serve as an important correlation criterion for the definition of the Jurassic/Cretaceous boundary. It allows us to overcome the problems with biostratigraphic scale correlations in the Tethyan and Boreal realms. Magnetostratigraphic results hitherto obtained from samples from the Jurassic/Cretaceous boundary strata in the Tethyan realm (cf. Lowrie & Channell 1983; Ogg et al. 1984, 1988, 1991; Márton 1986; Zeiss 1986) along with the results recently inferred from the localities of Brodno near Žilina, Slovakia, and Štramberk, Moravia (Houša et al. 1996a,b) stimulated detailed magnetostratigraphic research, particularly working out of the high-resolution magnetostratigraphic scales in other regions of the Tethyan realm. Such a scale has already been worked out for the locality of Brodno near Žilina, where two narrow reverse subzones were detected very precisely within the normal magnetozones M19 and M20, in addition to the normal and reverse magnetozones M17 through M21.

Two additional sections in the Tethyan realm were selected for high-resolution magnetostratigraphic research, i.e. sections in the Bosso Valley (Umbria, central Italy) and in the Río Argos (Subbetics, Spain). The studies in the Bosso Valley follow the already completed basic magnetostratigraphic research which indicated clearly defined magnetozones suitable for correlation with magnetic anomalies M19 through M14, or probably through M13 of the marine Mesozoic sequence M (Lowrie & Channell 1983). Suitable physical properties of rocks as well as an adequate geological setting comprise the fundamental premise for the working out of a high-resolution magnetostratigraphic scale at this locality. Another goal was to work out a magnetostratigraphic scale for a limestone-dominated Lower Cretaceous succession in the Río Argos (Caravaca) area, documented in much detail both geologically and paleontologically (Hoedemaeker & Leereveld 1995). Much attention was paid to the Río Argos section with respect to its high importance, good outcrops of the individual strata and their clear numbering in the field. However, it was at this section that serious problems resulting from remagnetization of limestones were encountered.

Progressive thermal demagnetization using the MAVACS apparatus (Příhoda et al. 1989) proved to be the most suitable tool for the inference of remanent magnetization components. The measured data were tested using multi-component remanence analysis and the separated remanence components combined with fold tests were statistically evaluated. The values of the volume magnetic susceptibility of samples subjected to thermal demagnetization were also registered so that the possible phase and mineralogical changes of magnetically active minerals could be determined at each step of the thermal demagnetization process. Magneto-mineralogical analysis and magnetic susceptibility anisotropy study of pilot samples were carried out. The statistically rich material (361 oriented hand samples from respective limestone beds) has unambiguously proved that the absolute majority of rock samples display post-tectonic and syn-tectonic magnetization with a large portion of the rocks having been totally remagnetized in the Neogene. It was also possible to determine the situation of the epicentrum of processes resulting in the maximum remagnetization during the reverse polarity of paleomagnetic field in the Neogene. Primary paleomagnetic directions were practically completely destroyed, although they are well reproducable at other or nearby localities with rocks of analogous age and composition (e.g. Cehegin, Carcabuey). The syn-tectonic magnetization was inferred on the basis of the study of the precision parameter k or of the semi-vertical angle of the confidence cone $\alpha_{95}$ (Fisher 1953) depending upon gradual changes in the dip of strata (ranging between maximum dip angles and the horizontal position). The components of syn-tectonic magnetization indicate a clockwise paleotectonic rotation. Analogous methodological and paleotectonic conclusions were reported from other localities in Spain, e.g. from the Betic orogen (Villalaín et al. 1996; Parés & Roca 1996). The aim of the presented study is to briefly highlight the main geophysical and paleotectonic conclusions as analogous problems may appear at other localities in the Tethyan realm.

## A brief outline of the geology of the studied region

The Lower Cretaceous Río Argos succession is situated in the frontal parts of the Subbetic Zone of the Betic Cordilleras (SE Spain) and crops out in several sections along the River Argos and its tributaries west of Caravaca. It is the most complete and best preserved Lower Cretaceous succession in the Betic Cordilleras. Detailed logs of the entire succession were constructed and all beds were numbered.

### *Lithology of the Río Argos Succession*

The part of the succession incorporated in this study is 1500 m thick and consists of a rather monotonous cyclic alternation of olive grey marly limestone beds and dark grey, shaly marlstone interbeds. In the micritic limestone beds and marlstone interbeds, clay is the main siliciclastic fraction. From the middle Valanginian part upwards, up to 1 % silt-sized quartz grains occur. In the upper Barremian and Aptian proximal sandstone turbidites are frequent. The lime fraction (for the upper Berriasian ranging between 58 and 83 % with a mean value of 72.5 %) consists almost entirely of coccolith and *Nannoconus* tests and their fragments, slightly encrusted by sparry calcite.

Diagenetic overprinting has been indicated: apart from mechanical compaction (80–90 % for the marlstone interbeds and 40–60 % for the limestone beds), differential dissolution and cementation has occurred giving rise to enhancement of the lithologic contrast of bedding and to nodular limestone beds.

The entire Lower Cretaceous Río Argos Succession was deposited in pelagic environments. Several paleo-ecological arguments (Hoedemaeker & Leereveld 1995) suggest that deposition occurred at a depth estimated to be in the order of 300–400 m. Many megafossils were pyritized and later limonitized.

### *Fossils and stratigraphy*

The Río Argos Succession is 1500 m thick and comprises the Berriasian up to the lower Aptian stages. 99 % of the megafossils consist of ammonites, either preserved as calcareous moulds or as limonitized steinkerns. Other megafossils are echinoids, brachiopods, belemnites, a few bivalves and a few gasteropods. The microfossils are foraminifers, dinoflagellate cysts, calpionellids, radiolarians, nannoconids and coccoliths.

The chronostratigraphy, biostratigraphy and sequence stratigraphy of the Río Argos Succession has been described in Hoedemaeker & Leereveld (1995). A cyclostratigraphic analysis of the Berriasian has been done by ten Kate & Sprenger (1989) and Sprenger & ten Kate (1992).

### *Geological setting and tectonic evolution*

The geology and tectonics of the region have been studied by Van Ween (1969) and Hoedemaeker (1974). They presented a detailed description of the geology of the region and geological maps. For the tectonic units of the Moratalla–Caravaca region see Fig. 1. The Lower Cretaceous Río Argos Succession forms part of the allochthonous Subbetic Zone, which mainly consists of pelagic deposits (with the exception of the Triassic and Lower Jurassic rocks). In Ser-

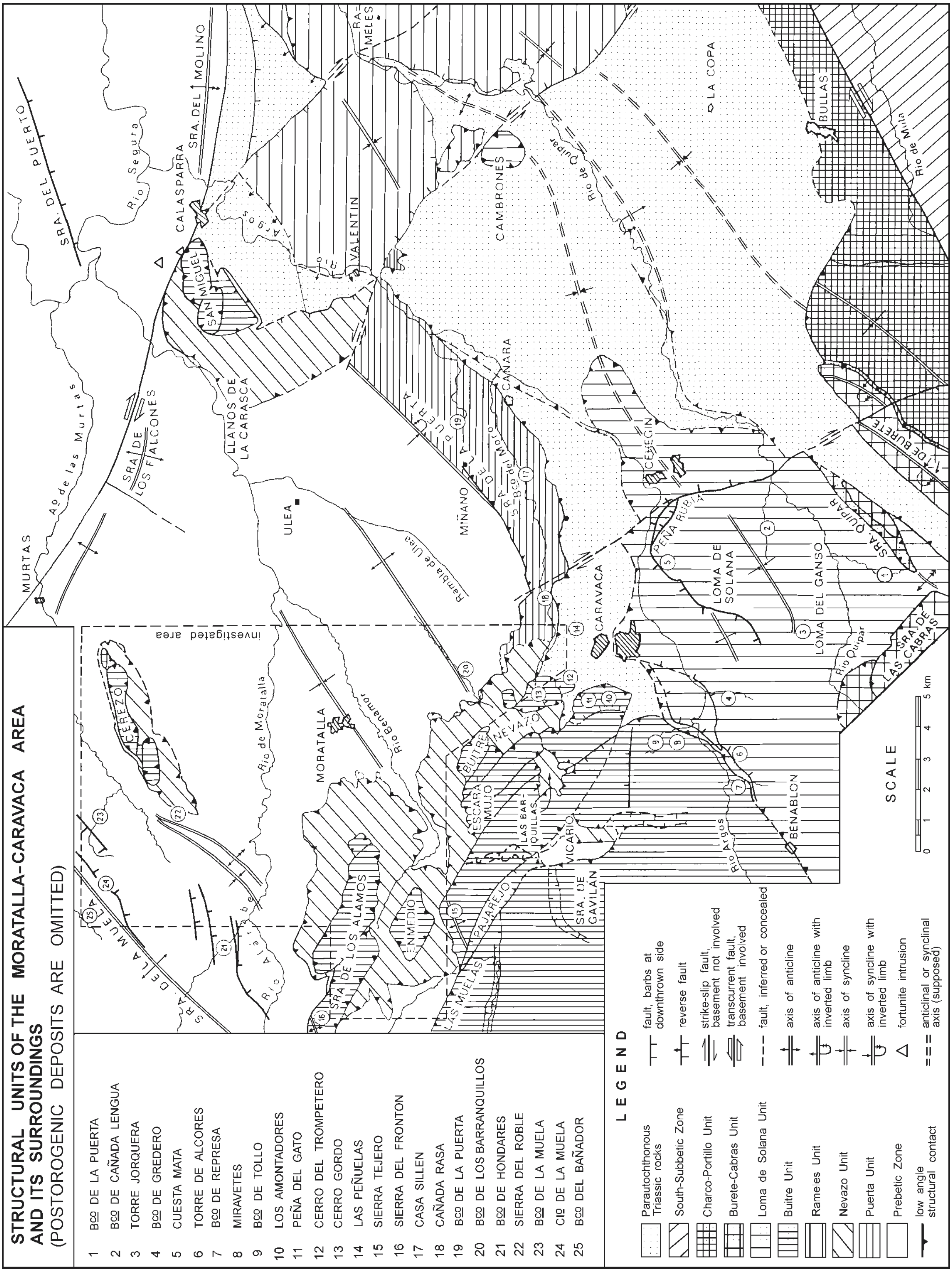


**Fig. 1.** Tectonic units of the Moratalla–Caravaca region.

ravallian time (10–14 Ma) the frontal parts of the Subbetic Zone thrusted northwestward over the autochthonous Prebetic Zone, which is mainly composed of rocks deposited in a neritic environment. The tectonic evolution of the Subbetic Zone of the Caravaca region can be characterized as a "décollement" process leading, through diapiric action of the gypsiferous Triassic rocks, to concentric folding of the Subbetic rocks above a detachment plane into box-folds that evolved either into diapiric folds (flower structures) or, when asymmetrical, into fold-overthrusts. The cores of the folds consist of Triassic rocks. The detachment plane is situated in the upper gypsiferous part of the parautochthonous Triassic rocks. The Paleozoic basement rocks did not take part in the thrusting. The primordial boxfolds started growing at the beginning of the Lutetian age, some 50 Ma ago.

The Río Argos Succession is situated in the frontal fold-overthrust (the Buitre Unit) of the Subbetic Zone where Jurassic carbonate rocks have thrusted at least 5 kilometers nothwestward over the deep, autochthonous basin-shaped syncline of Moratalla, which forms part of the Prebetic Zone. The Río Argos Succession forms the southeastern flank of the overthrusted fold (Fig. 2).

The deeper steep part of the overthrust fault is probably situated vertically below the Río Argos, along which the Lower Cretaceous succession is exposed. This fault may have some relation to a basement structure because of the presence of a small diabase intrusive body found 100 m north of the Cortijo de la Puerta piercing through the overturned part of the Prebetic Zone close to the overthrust fault (Hoedemaeker 1974, p. 96, enclosure 5). The age of this diabase is unknown but cannot be older than late Ypresian. This diabase has nothing to do with the diabase intrusives commonly found in the Triassic rocks, which are generally considered to be of Triassic age (Van Veen 1969, p. 104), but might be related to the late Neogene volcanic phase in SE Spain, during which small volcanoes were formed near Calasparra, 15 km to the northeast. This basement structure may approximately be parallel to the northeast-southwest strike of the overthrust fault. This basement structure would be vertically below the Lower Cretaceous outcrops along the Río Argos.

The Palaeozoic basement is divided into blocks bounded by northeast-southwest trending normal faults. These faults already existed in Berriasian time, and became active again

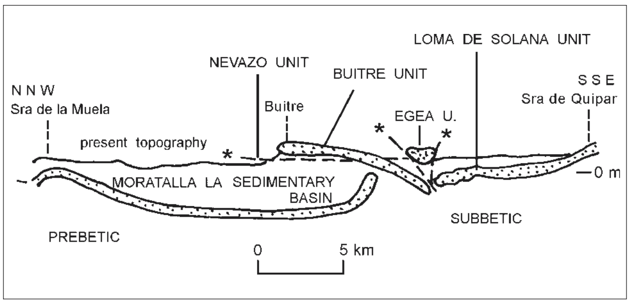


**Fig. 2.** Diagrammatic cross-section showing the tectonic structure of the relevant Jurassic strata in the Moratalla–Caravaca region. The Río Argos Succession is situated in the southern part of the Buitre Unit just north of the Egea Subunit, which is the frontal part of the Loma de Solana Unit.

in early Albian times (Hoedemaeker 1974, p. 187). From the detailed investigations of the stratigraphy of the Río Argos Succession by Hoedemaeker (field work from 1973 onward), it became clear that there is a gradual thinning followed by an abrupt thickening of the stratigraphic units when following them from west to east along the Río Argos. From this variation in thicknesses it can be concluded that there existed a roughly north-south trending submarine fault escarpment separating an eastern from a western Early Cretaceous sub-basin. This fault escarpment is tentatively interpreted as a reflection of a northwest-southeast trending basement fault, which would cross the basement structure that runs parallel to the strike of the overthrust fault.

## Collection of oriented rock samples, laboratory procedures

Altogether 361 oriented hand samples were collected from well defined limestone beds covering the epochs of the Berriasian, Valanginian, Hauterivian, Barremian and the Early Aptian. The individual intervals of the section across limestone beds are marked by Z, Y, M, N, P, A, Q2, Q'', S2, V2 and U as described by Hoedemaeker & Leereveld (1995). Field sampling was done under the supervision of Ph.J. Hoedemaeker and the individual oriented hand samples were numbered 1 to 361 from the Lower Berriasian to the Lower Aptian beds. In some cases, two samples were collected from a single bed (but from a different sampling site) for verification purposes. The repeated samples show these numbers: 94 (from bed Y 90), 98 (bed Y 102), 104 (bed Y 125), 110 (bed Y 148), 119 (bed Y 182), 123 (bed Y 197), 138 (bed Y 258), 139 (bed Y 261), 156 (bed Y 319), 174 (bed M 275), 177 (bed M 290), 211 (bed P 19), 216 (bed P 26), 220 (bed P 41), 236 (bed A 9), 237 (bed A 14), 246 (bed A 51), 266 (bed A 145) and 335 (bed V2 56). Time overlap is present in one part of the section, i.e., the samples were collected from two different parts of beds but of the same age: samples of Nos. 144 to 155 corresponding to beds 276 C to 319 of the Y section chronologically coincide with samples of Nos. 157 to 167 corresponding to beds 200 to 248 of the M section (see Fig. 3). For study purposes, seven oriented samples numbered 355 to 361 were taken from the bed A 154 (the uppermost Hauterivian). Basic magnetic data related to remanence components are given in Figs. 3 to 6 for the individual numbered samples. Numbers of studied strata are described in detail in the paper by Hoedemaeker & Leereveld (1995).

Laboratory procedures were selected to allow the separation of the respective remanence components and the determination of their geological-historical origin. Therefore, moduli and directions of natural remanent magnetization ($J_n$) and directions of the separated remanence components were measured. Zijderveld diagrams as well as graphs of normalized remanent magnetization and magnetic susceptibility values in relation to the progressive demagnetization temperature were also plotted for each of the samples. Minerals acting as carriers of the respective remanence components were determined from the inferred unblocking temperatures.

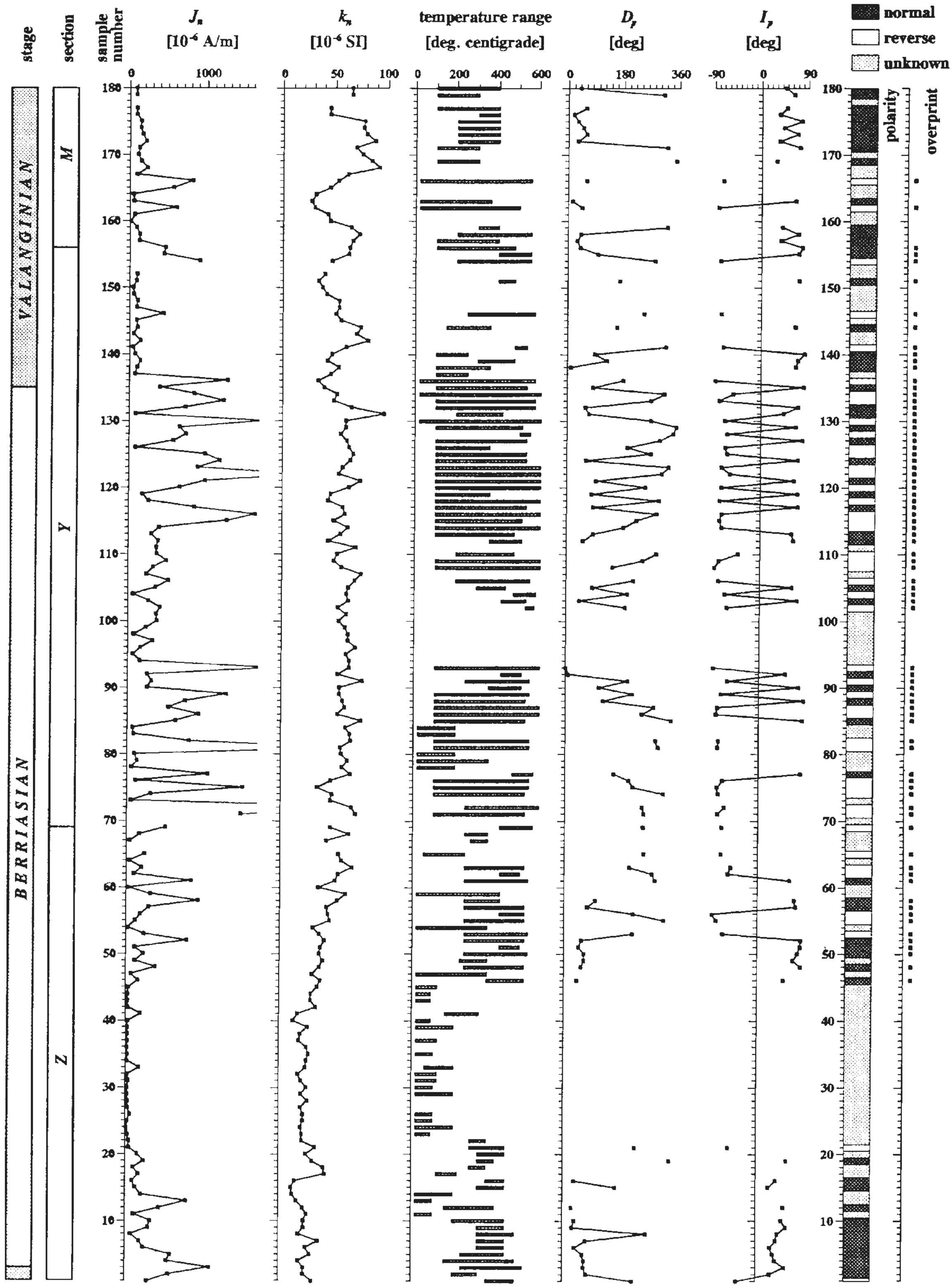


**Fig. 3.** The Río Argos section, Early Cretaceous limestone strata, samples Nos. 1 to 180. $J_n$ — modulus of natural remanent magnetization; $k_n$ — volume magnetic susceptibility of samples in natural state; temperature range — temperature interval in which the B-component of remanence was derived by multi-component analysis; $D_p$, $I_p$ — declination, inclination of B-component remanence; polarity — polarity of B-component remanence. Samples totally remagnetized are denoted by small full squares (overprint).

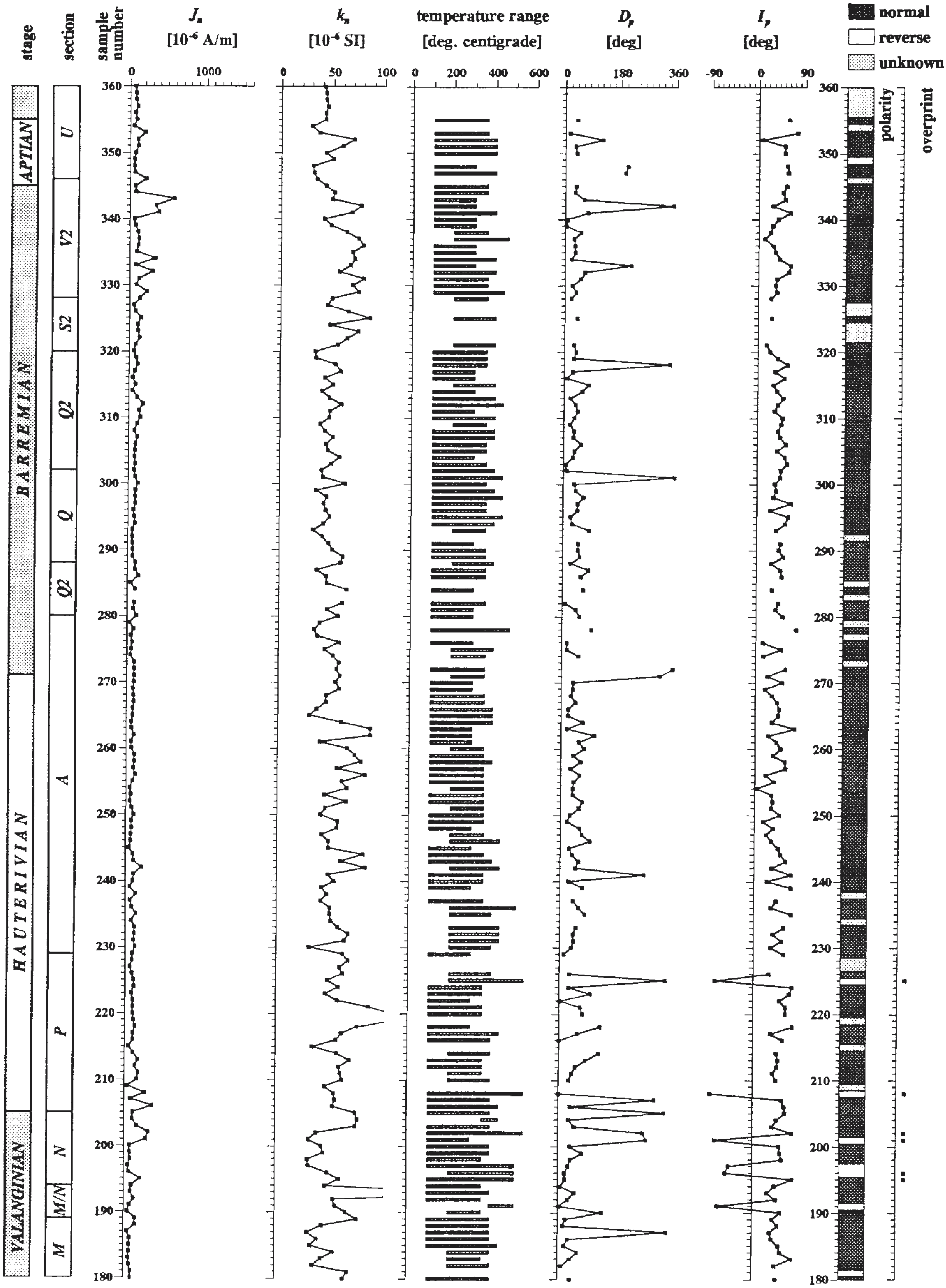


**Fig. 4.** The Río Argos section, Early Cretaceous limestone strata, samples Nos. 180 to 360. See legend to Fig. 3.

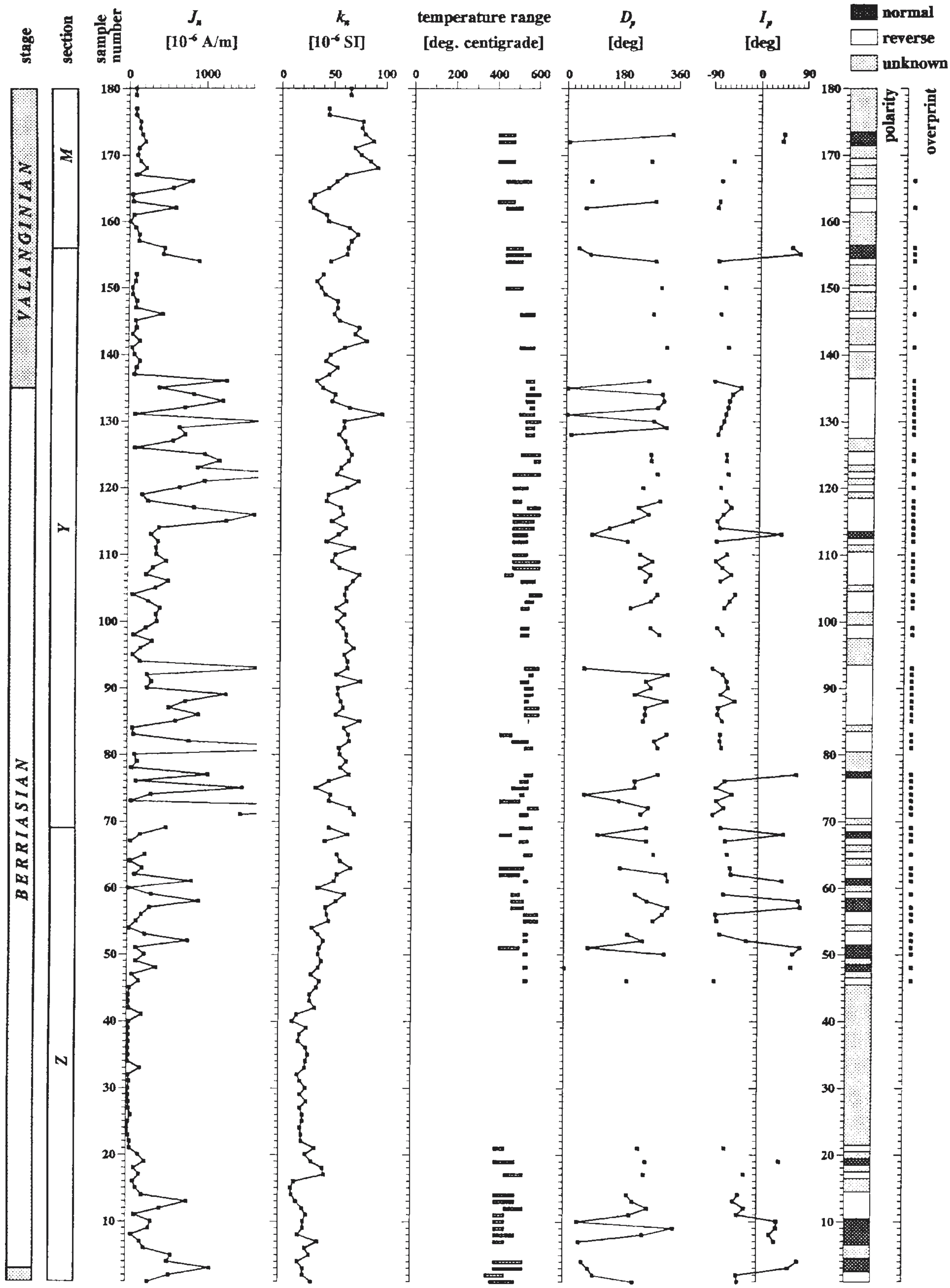


**Fig. 5.** The Río Argos section, Early Cretaceous limestone strata, samples Nos. 1 to 180. $J_n$ — modulus of natural remanent magnetization; $k_n$ — volume magnetic susceptibility of samples in natural state; temperature range — temperature interval in which the C-component of remanence was derived by multi-component analysis; $D_p$, $I_p$ — declination, inclination of C-component remanence; polarity — polarity of C-component remanence. Samples totally remagnetized are denoted by small full squares (overprint).

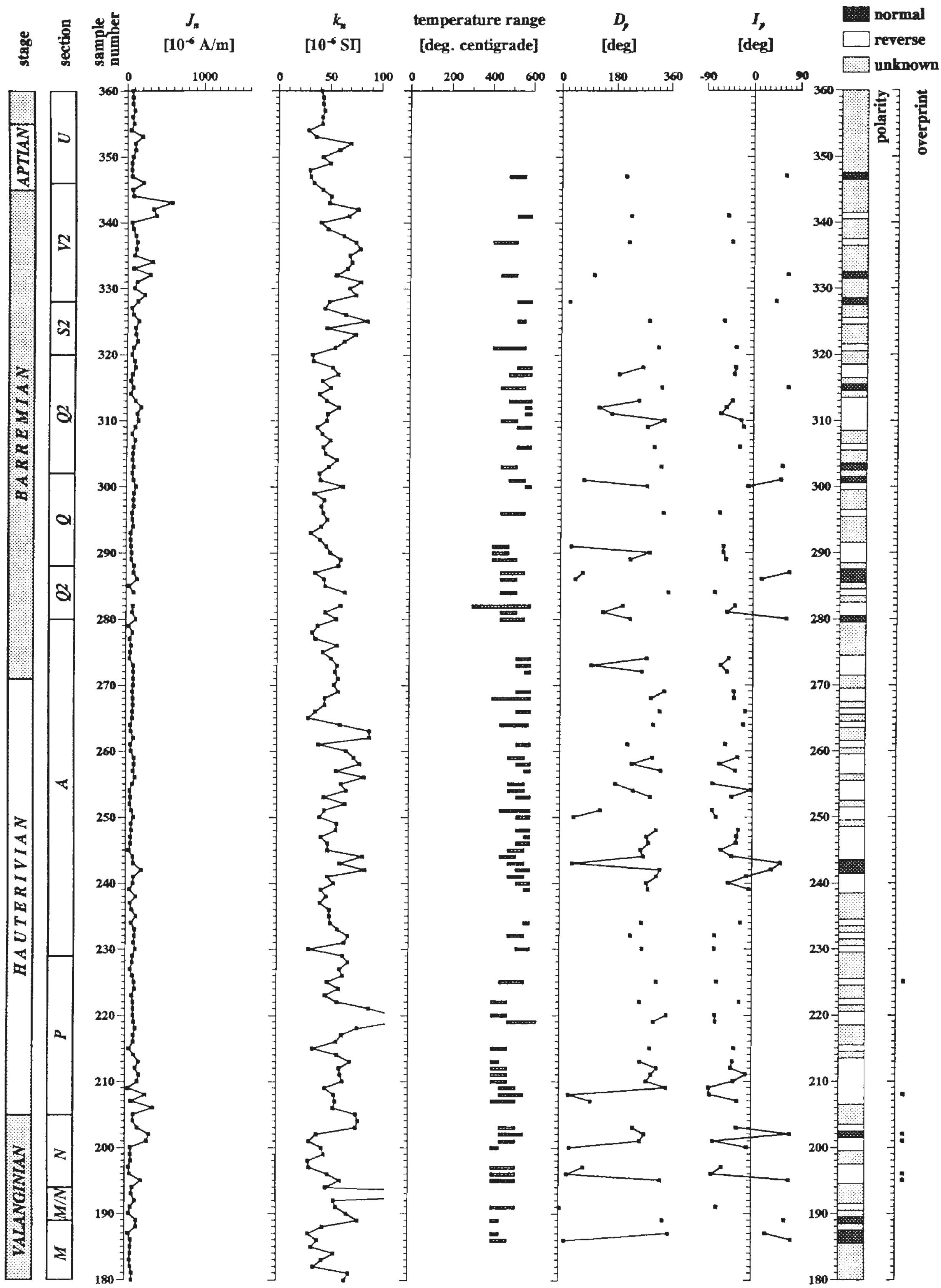


**Fig. 6.** The Río Argos section, Early Cretaceous limestone strata, samples Nos. 180 to 360. See legend to Fig. 5.

Cube-shaped laboratory specimens 20×20×20 mm in size were prepared from the oriented hand samples and measured by the JR-5 spinner magnetometer (Jelínek 1966). The specimens were subjected to progressive thermal demagnetization with the use of the MAVACS apparatus (Magnetic Vacuum Control System) ensuring the generation of a high magnetic vacuum in the environment of thermally demagnetized specimens (Příhoda et al. 1989).

Several specimens were also experimentally subjected to demagnetization by alternating field (A.F. procedures) using the Schonstedt GSD-1 apparatus. It was found suitable for the removal of viscous magnetization components but generally less effective than the MAVACS apparatus.

Phase and mineralogical changes frequently take place during thermal demagnetization, especially at higher temperatures. Therefore, the dependence of magnetic susceptibility on temperature was also measured. The values of volume magnetic susceptibility were measured on the KLY-2 kappabridge (Jelínek 1973).

Fifteen specimens were selected for detailed analyses with the aim of determining unblocking temperatures with a high precision and to verify the possible existence of a self-reversal phenomenon of remanence. These specimens were subjected to isothermal magnetization using a direct magnetic field to the state of saturation at the maximum magnetizing field intensity of 900 mT (9000 Oe). Specimens with saturated remanent magnetization were subjected to progressive thermal demagnetization.

Separation of the respective remanent magnetization components was done using multi-component analysis (Kirschvink 1980). Fisher's (1953) statistics were used for the calculation of the mean directions of $J_n$ and of the directions of the separated remanence components combined with fold tests. Temperature intervals in which the respective remanence components were inferred are also given in graphs in Figs. 3 to 6.

## The values of magnetic susceptibility and remanent magnetization

The values of the moduli of $J_n$ of the studied rocks in their natural state are exceptionally low, largely depending on the origin of magnetization. The values of volume magnetic susceptibility are also low but mostly show a smaller scatter than $J_n$ values. The samples of the analysed rocks can be classified into three categories according to the values of $J_n$ and $k_n$:

i) Exceptionally low magnetization values are indicated for samples of Nos. 23 to 45 (with the exception of anomalous samples of Nos. 33 and 41): mean values of $J_n = 0.26 \pm 0.09\times10^{-4}$ [A/m], $k_n = 24 \pm 5\times10^{-6}$ [SI], n = 21 (n being the number of samples). These samples were collected from weathered rocks, as also indicated by the low unblocking temperature values, see Figs. 3 and 5. Rocks of this type are not suitable for the multi-component remanence analysis.

ii) The second category of samples shows increased values of $J_n$. The mean values of $J_n = 6.13 \pm 6.36\times10^{-4}$ [A/m], $k_n = 55 \pm 12\times10^{-6}$ [SI], n = 85. This set includes samples of Nos. 46 to 156 and some other samples. These samples were totally remagnetized in the Neogene; they are marked by the overprint symbol (small full squares) in Figs. 3 to 6.

iii) The third category of samples shows lower values of $J_n$, although the values of susceptibility are identical with those of the preceding category. This set includes samples of Nos. 1 to 22 and 157 to 361 (exceptions are marked by the overprint symbols in Figs. 3 to 6). The mean values of $J_n = 1.34 \pm 1.35\times10^{-4}$ [A/m], $k_n = 53 \pm 21\times10^{-6}$ [SI], n = 224. As we shall see later, this group of samples contains syntectonic magnetization.

Two samples of totally remagnetized limestone (Nos. 120 and 121) with reverse and normal polarities of remanent magnetization are shown in Figs. 7 and 8 as examples. Whereas the unblocking temperature ranges between 540 and 580 °C in the vast majority of samples, samples of Nos. 120 and 121 show a somewhat higher unblocking temperature. The viscous remanence component can be removed by a 20 mT alternating field or by thermal demagnetization to 100 °C. The remagnetization components prevail in the temperature interval of 100–610 °C.

A typical example of a limestone sample with syn-tectonic magnetization is shown in Fig. 9. Remanent magnetization is of a relatively low value, showing three different components: the A-component corresponds to viscous magnetization, the B-component is a normal one (in interval of 100–520 °C) and the C-component is a reverse one (in temperature interval of 540–580 °C). The C-component has a very low amplitude; it was inferred with a low confidence level in many cases.

The C-component was inferred at higher demagnetization temperature intervals, above 400 to 500 °C and is largely reversely polarized. To verify the possible origin of a self-reversal of remanence and to determine the unblocking temperatures more precisely, 15 pilot samples representing both totally remagnetized samples and samples with syn-tectonic magnetization were subjected to the following tests: the selected samples were progressively isothermally magnetized by a direct field of intensities of 5, 10, 20, 100 and 900 mT. The values of saturated remanent magnetization ($J_s$) reached high values — several tens to hundreds of $10^{-3}$ [A/m]. Normalized values of saturated remanent magnetization and of magnetic susceptibility for four samples are given as examples in Fig. 10. The absence of self-reversal of remanence was proved for all fifteen pilot samples and magnetite was determined as the principal carrier of remanent magnetization on the basis of unblocking temperatures. A higher unblocking temperature above 600 °C was determined in only one sample (totally remagnetized), indicating an admixture of other minerals ($\eta$- or $\alpha$-$Fe_2O_3$?).

## Directions of $J_n$ (NRM) and of separated B- and C-components of remanent magnetization

The distribution of $J_n$ directions suggests that the studied limestone beds were either totally or partially remagnetized. Fig. 11 shows the $J_n$ directions of limestone beds not corrected for dip. Three sets of $J_n$ directions are very similar but the set in Fig. 11c shows no reverse directions of $J_n$ with

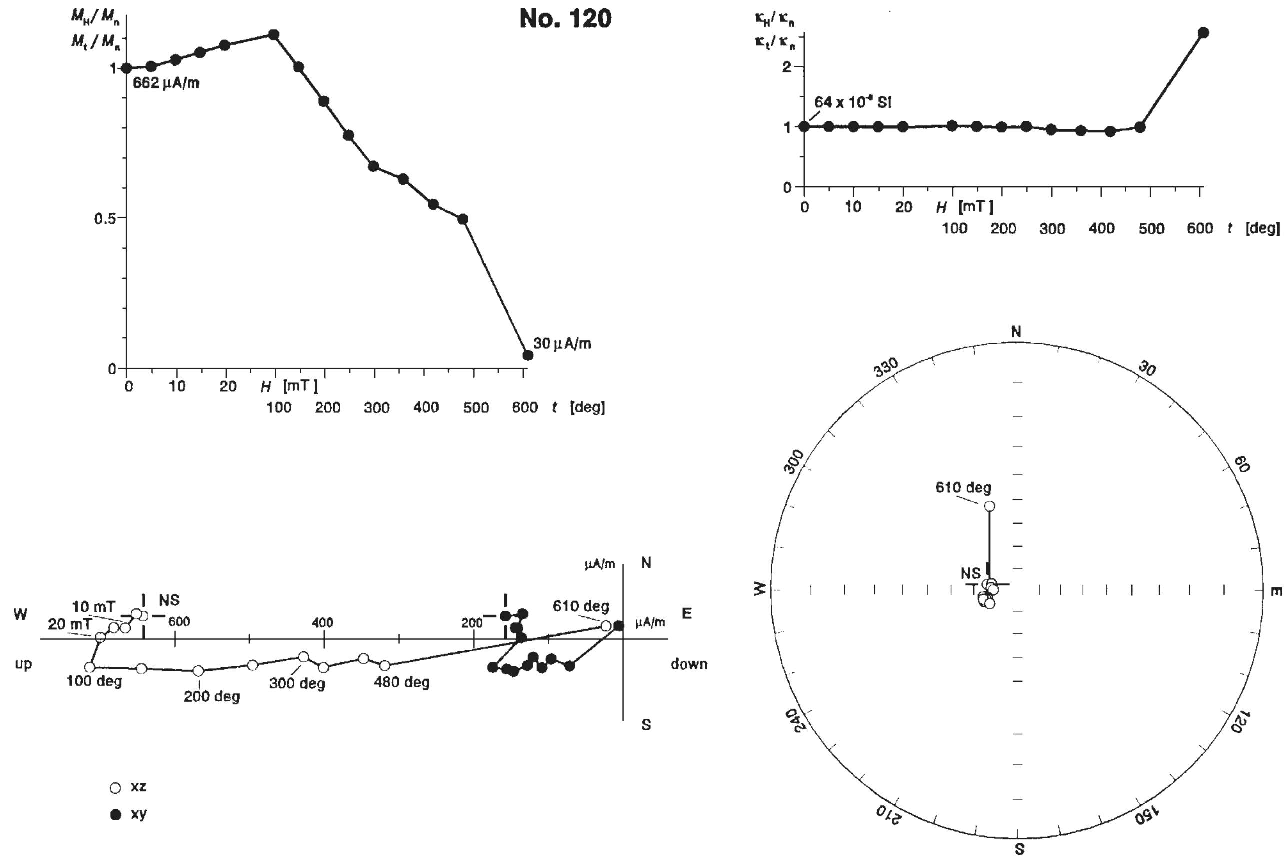


**Fig. 7.** A limestone sample No. 120 with reverse polarity and totally remagnetized during the Neogene, results of combined (A.F. and thermal) demagnetization. Upper part of the figure: $M_H$, $M_t$ — remanent magnetic moment of a sample demagnetized by alternating field (H, mT), at temperature t (°C); $M_n$— remanent magnetic moment of a sample in natural state (NS); $M_H/M_n$, $M_t/M_n$ and $k_H/k_n$, $k_t/k_n$ are normalized values of remanent magnetic moment and of volume magnetic susceptibility, respectively. Lower part of the figure: Zijderveld diagram, solid circles represent projections on the horizontal plane and open circles represent those on the N-S vertical plane. Stereographic projection, NS — sample in natural state (NRM), open (solid) circles represent projection on the upper (lower) hemisphere.

declination around 180°. This set includes samples with somewhat higher values of declination (D). As it is obvious from the text below, these differences result from a lower degree of remagnetization of rocks shown in Fig. 11c.

All the collected samples (n = 361) were subjected to progressive demagnetization at relatively dense steps. The Schonstedt GSD-1 apparatus was used for alternating field demagnetization and the MAVACS apparatus was used for thermal demagnetization (Příhoda et al. 1989). At the beginning of laboratory experiments, a relatively small set of samples was subjected to thermal demagnetization at temperatures of 60, 90, 120, 160, 200, 240, 280, 320, 360, 400, 450, 500, 540, 560 and 590 °C. A larger portion of samples was subjected to a combined demagnetization by alternating field of 50, 100, 150, 200 mT and by thermal field at temperatures of 100, (150), 200, (250), 300, 360, 400, 440, 480, 520, 560, 580 or 590 °C, (610 or 620, 650, 680 or 690 °C). The remaining samples were demagnetized only thermally. Temperatures applied to some selected sets of samples are given in brackets.

The directions of remanent magnetization inferred by the above given procedures were tested using a multi-component analysis (Kirschvink 1980). Generally, the samples showed three remanence components: A, B and C. The A-components are mostly of viscous or chemoremanent (weathering) origin. They can be removed by an alternating field to 20 mT or by a thermal field to 100 °C. For a better understanding of the remagnetization problem, the temperature intervals at which the directions of the B- and C-components were separated are plotted in Figs. 3 to 6.

On the basis of the B- and C-components direction analysis, the studied rocks can be divided into two groups of rocks of post-tectonically totally remagnetized and syn-tectonically remagnetized.

The normal and reverse B-component directions of the totally remagnetized samples (marked by small full squares in Figs. 3 and 4) form two well-defined sets of samples with fisherian distribution. The directions not corrected for the dip of strata (in situ directions) are shown in Fig. 12, and the mean directions calculated after Fisher (1953) for the 95 % probability level along with the corresponding paleomagnetic pole position are summarized in Table 1, see Fig. 13. The data imply that the rocks of the studied samples were totally remagnetized in the Neogene. The situation of the epicentrum of processes causing the overprint of B-components is located in the area of collection of samples of Nos. 46 to 156. The analysis of C-components further revealed that numerous samples were totally remagnetized during a

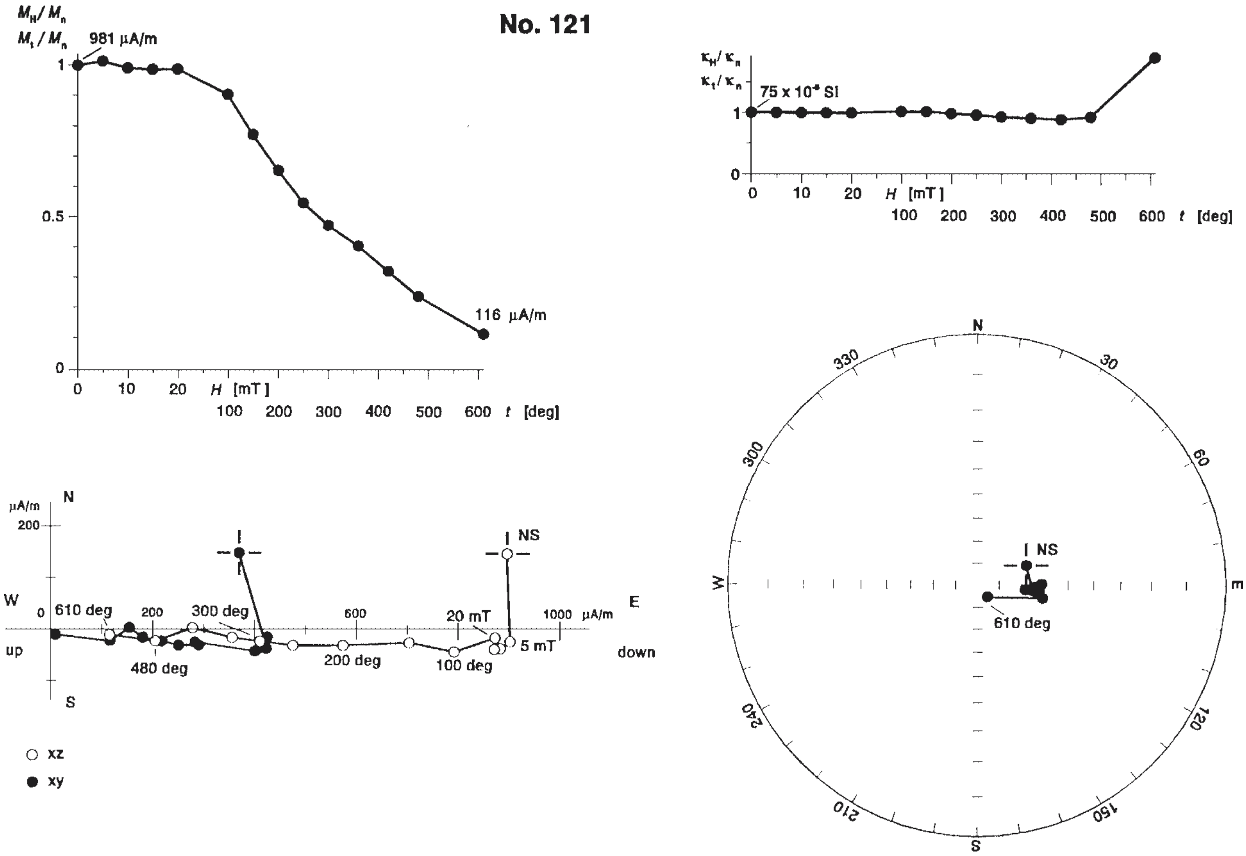


Fig. 8. A limestone sample No. 121 with normal polarity and totally remagnetized during the Neogene. See legend to Fig. 7.

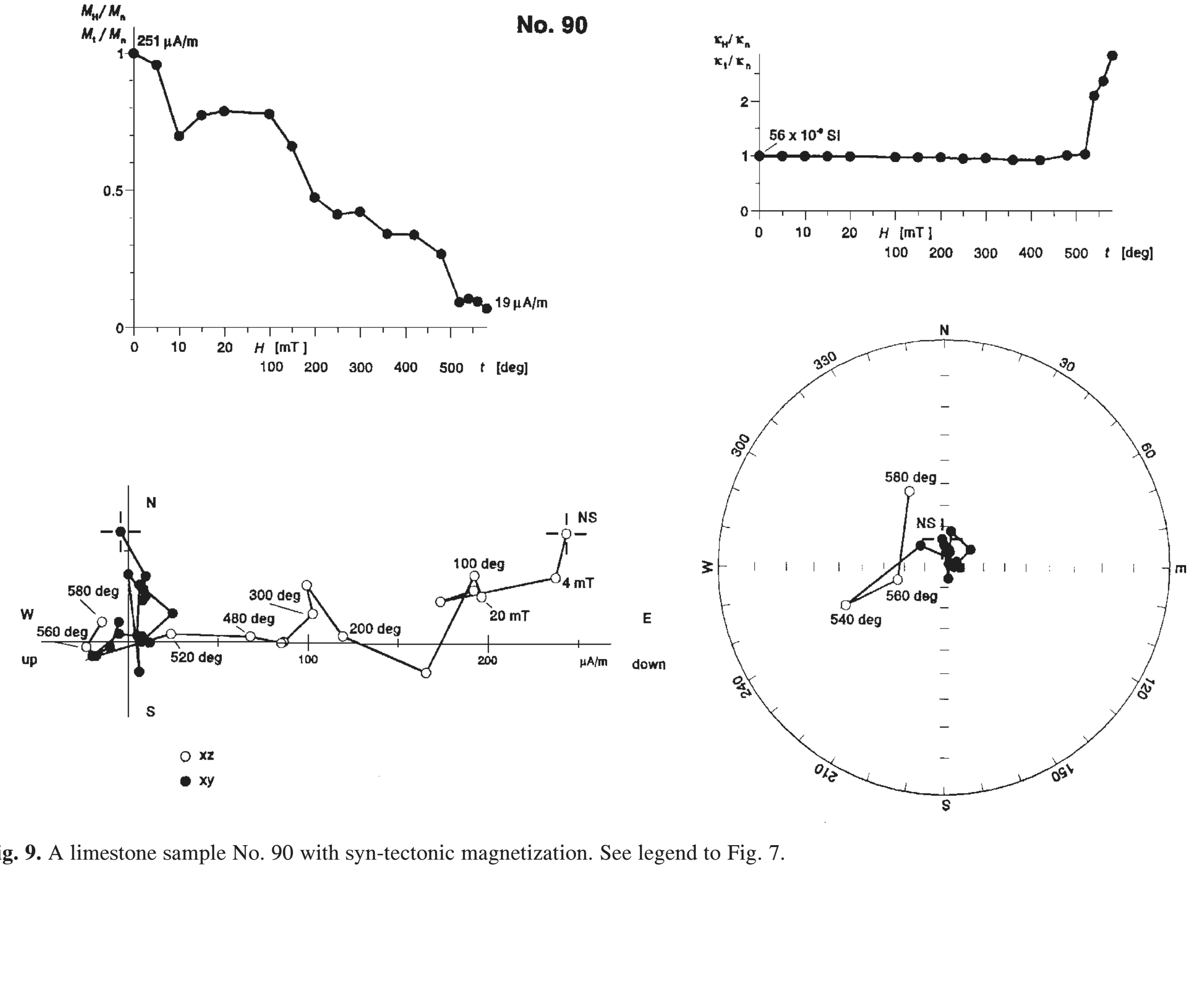


Fig. 9. A limestone sample No. 90 with syn-tectonic magnetization. See legend to Fig. 7.

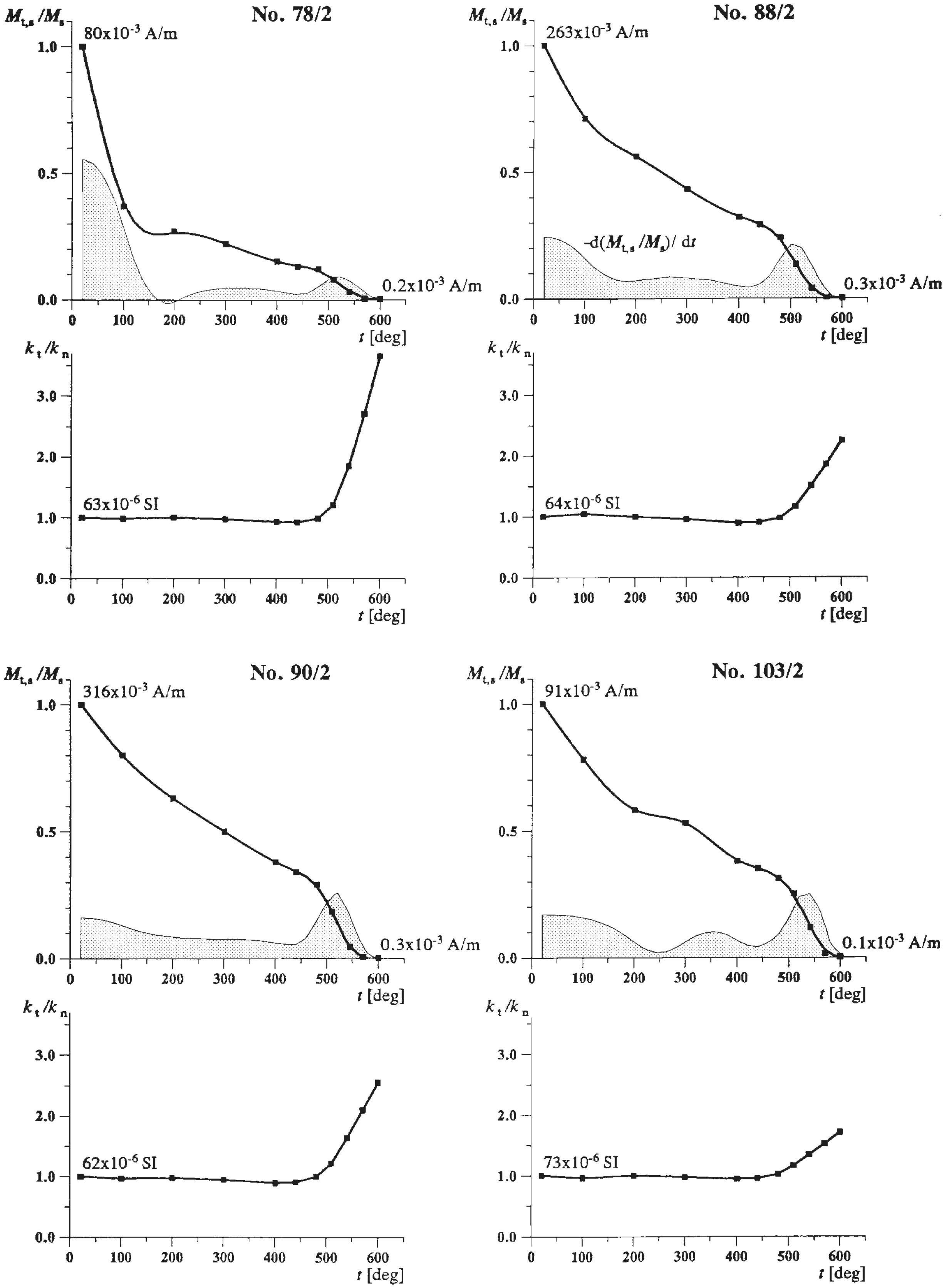


**Fig. 10.** Results of the thermal demagnetization of four pilot samples (Nos. 78/2; 88/2; 90/2; 103/2) subjected to isothermal magnetization up to the saturation state prior to thermal treatment. $M_{t,s}$ — remanent saturation magnetic moment demagnetized at temperature t (°C); $M_s$ — remanent saturation magnetic moment at room temperature (20 °C). $M_{t,s}$ / $M_s$ and $k_t/k_n$ are normalized values of remanent magnetic moment and of volume magnetic susceptibility, respectively.

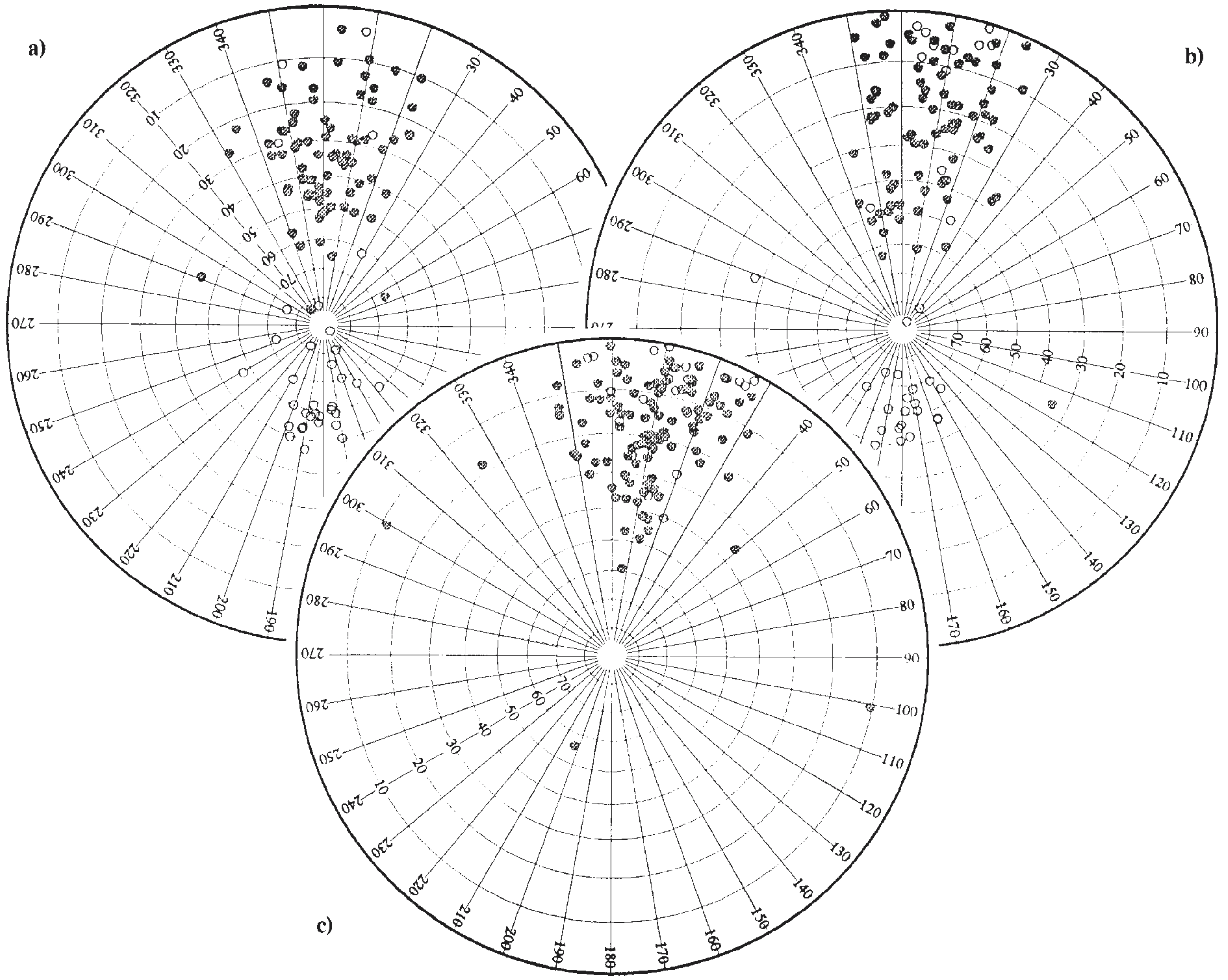


**Fig. 11.** Directions of natural remanent magnetization ($J_n$) not corrected for dip of rocks (in situ directions): a) set of samples Nos. 1–114; b) set of samples Nos. 115–229; c) set of samples of Nos. 231–355. Stereographic projections of directions onto lower (upper) hemisphere are denoted by small full (open) circles.

reverse polarity of the paleomagnetic field in the Neogene. The epicentrum of processes resulting in the overprint of C-components is located in the area of collection of samples of Nos. 81 to 154, which further restricts the area of processes leading to total rock remagnetization. Table 2 parallels Table 1 but the data summarized relate to the C-components; the calculated results confirm the Neogene age of the overprint. In both tables, the reverse directions were transformed into normal directions due to the calculation of the paleomagnetic pole position.

The directions of the B-components of remanence of the remaining samples were also statistically evaluated (Fisher 1953) with the exclusion of totally weathered samples (of samples with unblocking temperature below 100 °C) and of totally remagnetized samples (shown on Fig. 12). The following results were obtained: $\alpha_{95}$ = 4.7°; k = 6.2; n = 176

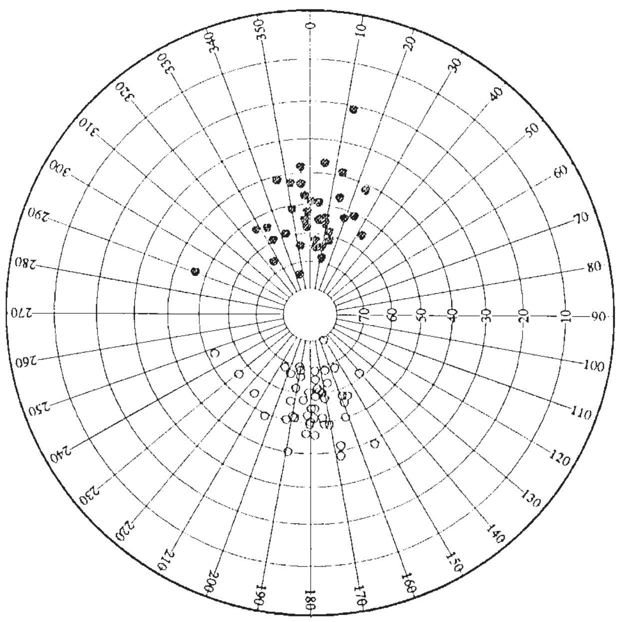

**Fig. 12.** Directions of B-components of remanence of limestone samples totally remagnetized during the Neogene, not corrected for dip of rocks (in situ directions). These samples are denoted by small full squares in Figs. 3 and 4.

**Table 1:** The Río Argos. Mean paleomagnetic direction and pole position calculated from B-components of totally remagnetized limestone samples.

| Mean geogr. coordinates | | Mean direction | | | | | Pole position | | Oval of confidence | |
|---|---|---|---|---|---|---|---|---|---|---|
| Lat. [°N] | Long. [°E] | Decl. [°] | Incl. [°] | $\alpha_{95}$ [°] | k | N | Paleo-lat. | Paleo-long. | dm [°] | dp [°] |
| 38.1 | 358.1 | 359.3 | 56.2 | 2.8 | 31.8 | 84 | 88.6°N | 200.8°E | 4.0 | 2.9 |

**Table 2:** The Río Argos. Mean paleomagnetic direction and pole position calculated from C-components of totally remagnetized limestone samples.

| Mean geogr. coordinates | | Mean direction | | | | | Pole position | | Oval of confidence | |
|---|---|---|---|---|---|---|---|---|---|---|
| Lat. [°N] | Long. [°E] | Decl. [°] | Incl. [°] | $\alpha_{95}$ [°] | k | N | Paleo-lat. | Paleo-long. | dm [°] | dp [°] |
| 38.1 | 358.1 | 2.8 | 60.2 | 4.1 | 15.8 | 82 | 86.3°N | 32.7°E | 6.2 | 4.7 |

for samples not corrected for the dip of strata (in situ directions) and $\alpha_{95} = 4.5°$; k = 6.7; n = 176 for samples corrected for the dip of strata. The differences in the calculated values are statistically not significant. Table 3 summarizes the mean values of declination (D), inclination (I) of remanence, $\alpha_{95}$ and k for samples not corrected for the dip of strata (correction 0 %) and for samples corrected for the dip of strata (correction 100 %) as well as for transitional dip corrections at 10 to 90 %. The presented results indicate a syn-tectonic origin of B-components of remanence in this sample set. It is worth mentioning that with the exception of three samples the B-components are exclusively normally polarized, see Figs. 14 and 15. This a priori excludes the syn-sedimentary origin of the B-components of remanence.

## Study of anisotropy of magnetic susceptibility

The magnetic susceptibility of a rock is the ratio of induced magnetization to applied magnetic field. The anisotropy of magnetic susceptibility (AMS) can be described as a second-order tensor, which defines the susceptibility ellipsoid, with maximum (K1), intermediate (K2) and minimum (K3) principal axes defined by their magnitude and direction.

AMS in rocks can basically reflect: a) shape anisotropy, caused by the alignment of elongated grains; b) crystalline anisotropy, arising from the alignment of crystal axes. At low magnetic fields (0.1 mT), the susceptibility anisotropy of magnetite is controlled by the shape of the grain as long as the grains are not interacting. Hematite, like the paramagnetic (micas, hornblende, chlorite) and the diamagnetic (plagioclase,

**Table 3:** The Río Argos. Mean directions of B-components of remanence of samples with syntectonic magnetization.

| Corr. for dip [%] | Mean directions | | $\alpha_{95}$ [°] | k | n |
|---|---|---|---|---|---|
| | Decl. [°] | Incl. [°] | | | |
| 100 | 38.9 | 49.2 | 4.46 | 6.67 | 176 |
| 90 | 36.5 | 46.7 | 4.45 | 6.69 | 176 |
| 80 | 34.3 | 44.2 | 4.45 | 6.70 | 176 |
| 70 | 32.2 | 41.5 | 4.45 | 6.69 | 176 |
| 60 | 30.3 | 38.7 | 4.46 | 6.67 | 176 |
| 50 | 28.5 | 35.8 | 4.48 | 6.62 | 176 |
| 40 | 26.9 | 32.9 | 4.50 | 6.56 | 176 |
| 30 | 25.3 | 30.0 | 4.53 | 6.48 | 176 |
| 20 | 23.9 | 27.1 | 4.57 | 6.39 | 176 |
| 10 | 22.6 | 24.3 | 4.61 | 6.29 | 176 |
| 0 | 21.4 | 21.5 | 4.66 | 6.19 | 176 |

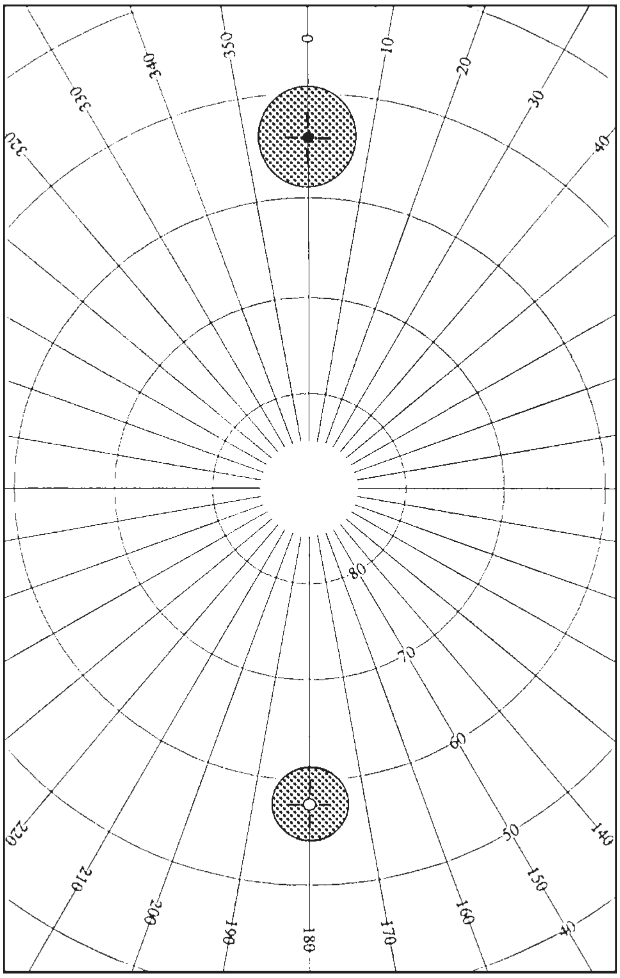


**Fig. 13.** Mean directions of B-components of samples described in Fig. 12. The mean directions denoted by solid or open crossed circles and circumscribed by circles of confidence were calculated according to Fisher (1953) at the 95 % probability level.

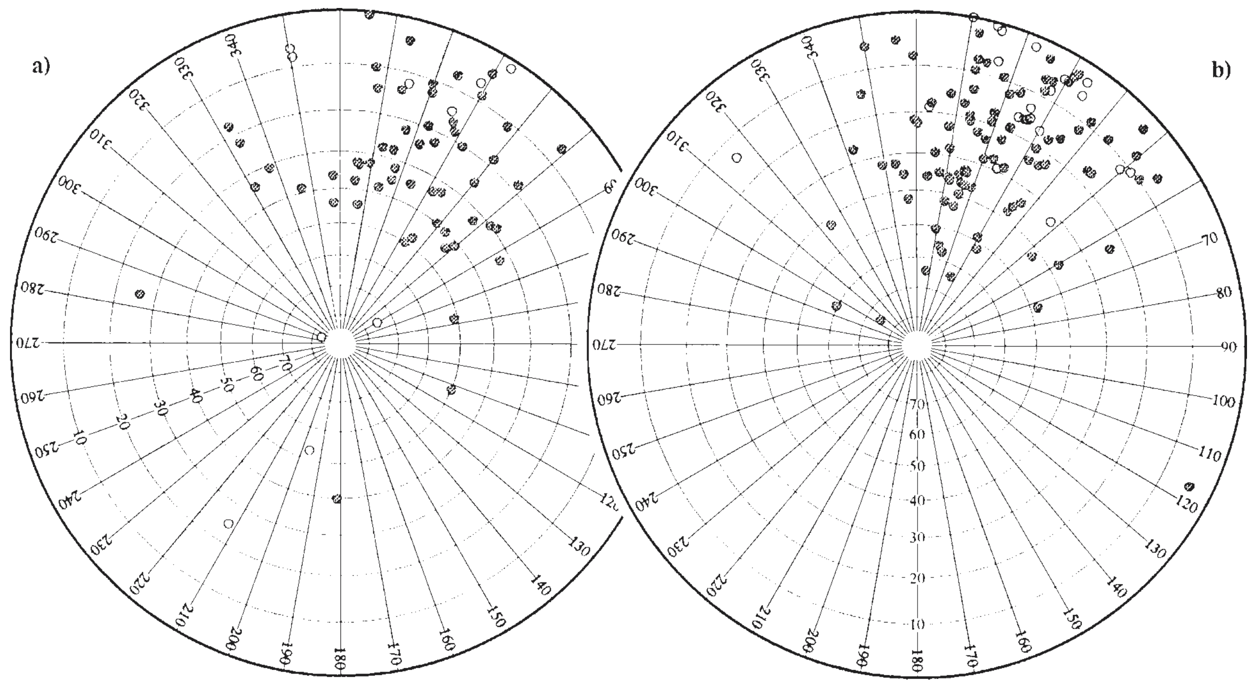


**Fig. 14.** The directions of B-components of remanence of partially remagnetized samples (with syn-tectonic remanence), not corrected for dip of rocks (in situ directions). a) From the set of samples Nos. 1–229. b) From the set of samples Nos. 231–335.

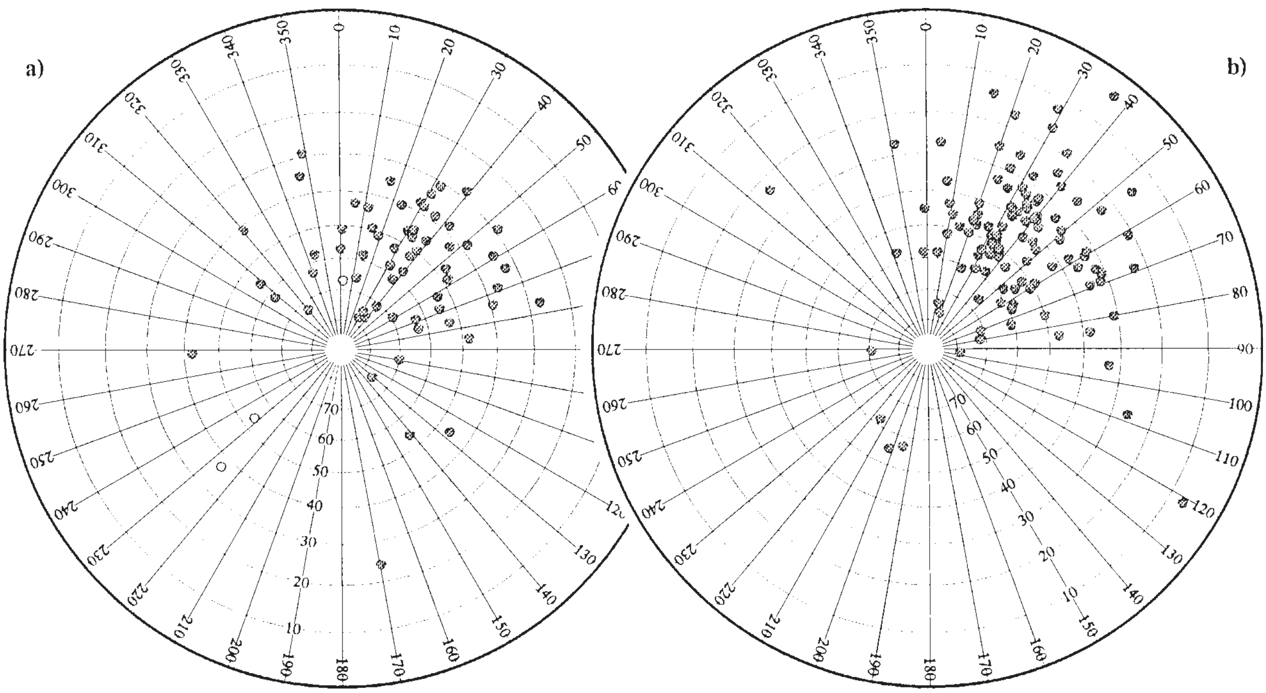


**Fig. 15.** Directions of B-components of samples described in Fig. 14, but corrected for dip of rocks.

quartz, calcite) rock-forming minerals, yields a component of magnetic fabric to the rock that is influenced primarily by the crystallographic alignment of the anisotropic grains.

Ten samples of totally remagnetized limestones and ten samples of partially remagnetized limestones (with syn-tectonic magnetization) were selected for study of the anisotropy of magnetic susceptibility using the method of Jelínek (1977). The Anisotropy of Magnetic Susceptibility (AMS) was measured using the Kappabridge KLY2.02 (Geofyzika Brno), which is based on measuring the so-called directional susceptibilities, corresponding to certain directions in the rock specimen. It would be sufficient to measure directional susceptibilities in six suitably chosen directions since the susceptibility tensor is symmetrical and thus has six independent components. Nevertheless, Jelínek (1977) developed a method according to which the measurement is per-

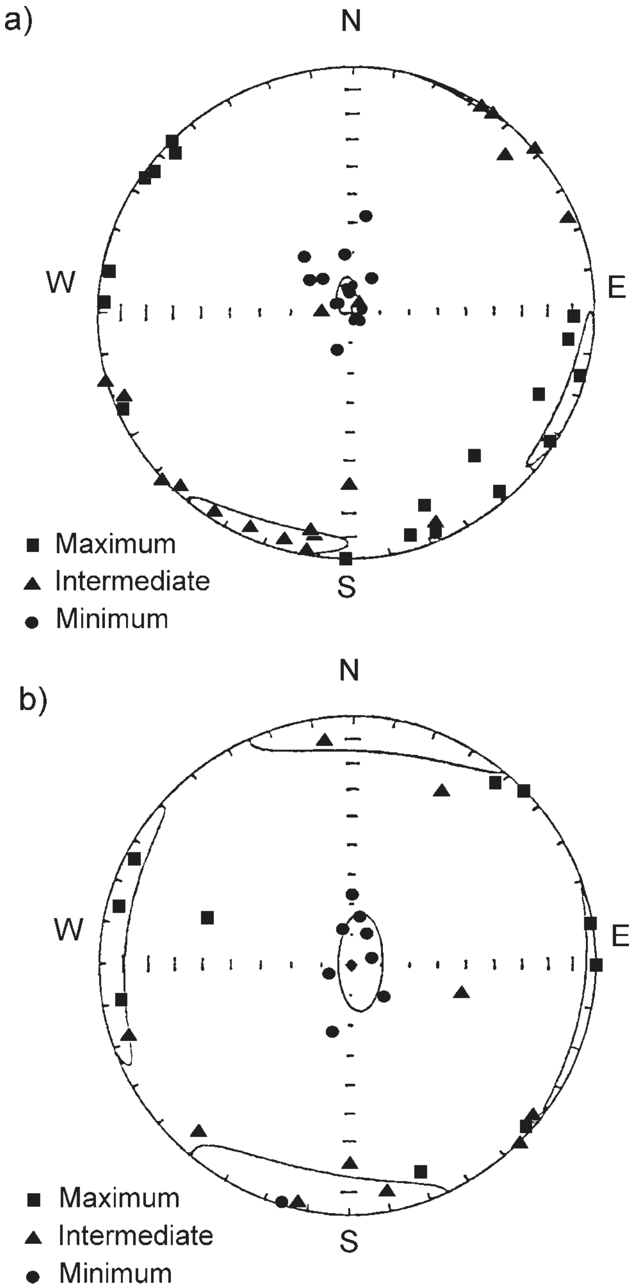


**Fig. 16.** Equal area projection of AMS principal axes for all measured samples: a) samples of limestone strata totally remagnetized in the Neogene (with post-tectonic magnetization); b) samples of limestone strata with syn-tectonic magnetization. Ellipses indicate the confidence level at 95 %. Squares — maximum principal axes. Triangles — intermediate principal axes. Dots — minimum principal axes.

formed in fifteen different positions and the elements of the susceptibility tensor are then determined by computer using a least squares method. An ellipsoid defined by the maximum, intermediate and minimum susceptibilities (K1 > K2 > K3) can be associated to the symmetrical tensor. The aim of this study was to verify whether the samples from both groups of limestones show similar or different parameters related to the anisotropy of magnetic susceptibility.

The fabric of limestones in both groups of samples shows the same features: the axes of minimum anisotropy are vertical (normal to the bedding) and the axes of maximum and intermediate anisotropy are contained within the bedding plane (Fig. 16). The maximum axes are roughly grouped, along WNW–ESE directions. This could reflect either an original paleocurrent or an extension direction due to the Tertiary compression that affected the region under study. In any case, the fabric is dominantly sedimentary: the maximum axes are vertical and normal to bedding. Another important feature is that the magnetic ellipsoids for all the samples are oblate. This means that foliation dominates over lineation, which is very common for sedimentary-type fabrics.

The values of bulk susceptibility (see Figs. 3 to 6) are very low, indicating both the influence of the diamagnetism component (calcite) and the low concentration of ferro- and paramagnetic minerals.

## Discussion to possible geological causes of the remagnetization

The décollement tectonics and the diapiric folding of the Buitre Unit do not involve large stresses. The stresses involved were mainly transmitted through the competent Jurassic carbonate rocks and not through the incompetent Cretaceous marls that were riding piggy-back upon the Jurassic carbonates. This also applies for the adjacent Loma de Solana Unit a few kilometers to the south, where the Cretaceous marls are not remagnetized. This means that extreme stresses cannot be regarded as the cause of the remagnetization of the rocks.

Thermal causes for the remagnetization also cannot be taken into consideration, because the delicate dinoflagellate cysts are still nicely preserved. They would immediately be destroyed by the slightest heating and by weathering.

If the interpretations of the basement structures in the Paleozoic basement are correct, it would imply that there would be a crossing of basement faults approximately below the frontal Buitre Unit of the Subbetic Zone. This may perhaps be the site of the remagnetization described in this paper.

## Principal results

The Early Cretaceous strata of limestones at the locality of the Río Argos were subjected to relatively extensive laboratory tests aimed at the inference of magnetostratigraphic data. However, the obtained results clearly show that the limestones were either syn-tectonically remagnetized or totally post-tectonically remagnetized in the Neogene. With respect to growing activities in magnetostratigraphy in other regions of the Tethyan realm, it is worth mentioning the main methodological results:

**i)** The vast majority of the studied limestone samples show three components of remanence A, B and C. The A-components are of viscous or chemoremanent origin (effects of weathering) and were inferred in the temperature intervals below 100 °C. The B-components were mostly inferred in temperature intervals of 100 to 400 °C, see Figs. 3 and 4. The C-components of remanence could be inferred for a considerable number of samples in temperature intervals of 400 to 580 °C, see Figs. 5 and 6. The C-components of weakly magnetic, syn-tectonically remagnetized limestone samples show a large scatter and, therefore, could not be used for a reliable interpretation. However, the C-components of more strongly magnetic, totally remagnetized samples could be used for interpretation, see Table 2.

**ii)** A relatively small number of samples proved to be intensely weathered. These samples were not used for the multi-component analysis. The samples of intensely weathered limestones are characterized by unblocking temperature values below 100 °C, see samples of Nos. 23 through 45 (except for samples of Nos. 33 and 41) in Fig. 3. The magnetic susceptibility of these samples is also markedly lower than in all other samples.

**iii)** Samples Nos. 46 to 156 and several other samples marked by small full squares in Figs. 3 to 6 represent sections of limestone beds totally remagnetized in the Neogene. The most intense remagnetization occurred at a reverse polarity of paleomagnetic field. The epicentrum of processes resulting in total remagnetization of limestone beds is located in the area between samples Nos. 46 to 156, i.e., between the beds Z 212 and Y 319.

**iv)** Apart from the samples listed under ii) and iii), the limestone samples from the whole Río Argos section indicate a syn-tectonic remanent magnetization. This magnetization was inferred from the study of precision parameter k or of the semi-vertical angle of the confidence cone $\alpha_{95}$ (Fisher 1953) in dependence upon different dip angles of strata, see Table 3. The B-components of syn-tectonic remanent magnetization indicate a clockwise paleotectonic rotation, see Figs. 14 and 15.

**v)** Magnetite with a well-defined unblocking temperature proved to be the carrier of remanent magnetization in the vast majority of massive limestone samples from the Río Argos locality. Higher unblocking temperatures above 600 °C were recorded in only a few limestone samples with increased remanent magnetization totally remagnetized in the Neogene. These temperatures indicate a possible admixture of some other minerals ($\eta$- or $\alpha$-$Fe_2O_3$?). Similar magnetic properties are shown by Mesozoic limestones with magnetite admixture in the Tethyan realm, which are mostly suitable for magnetostratigraphic studies. Petromagnetic and paleomagnetic analyses of limestones from the Río Argos locality represent a typical case history: magnetite-carrying fresh and massive limestones were remagnetized to such a degree that they completely lost the components of remanent magnetization syngenetic with the rock. These limestones macroscopically display no signs of thermal, hydrothermal, chemical, dynamo-metamorphic or other alterations. Similar examples of remagnetization of Mesozoic limestones were also pointed out by other authors (e.g. Villalaín et al. 1996; Parés & Roca 1996) and analogous cases could undoubtedly pose a certain danger during routine magnetostratigraphic studies. The geological cause of the remagnetization of limestones at the Río Argos locality remains unexplained.

**Acknowledgements:** The authors of this Report wish to thank the Netherlands Oil Company for financial support. J.M. Parés is grateful to the Spanish authorities for support within the E.C. Project No. CI1-CT94-0114.

## References

Fisher R., 1953: Dispersion on a sphere. *Proc. Roy. Soc., A,* 217, 295–305.

Hoedemaeker Ph.J., 1974: Olisthostromes and other delapsional deposits, and their occurrence in the region of Moratalla (Prov. of Murcia, Spain). *Scripta Geologica*, 19, 1–207.

Hoedemaeker Ph.J. & Leereveld H., 1995: Biostratigraphy and sequence stratigraphy of the Berriasian-lowest Aptian (Lower Cretaceous) of the Río Argos succession, Caravaca, SE Spain. *Cretaceous Research,* 16, 195–230.

Houša V., Krs M., Krsová M. & Pruner P., 1996a: Magnetostratigraphy of Jurassic-Cretaceous limestones in the Western Carpathians. In: Morris A. & Tarling D.H. (Eds.): Palaeomagnetism and Tectonics of the Mediterranean Region. *Spec. Publ. (Geol. Soc. London),* 105, 185–194.

Houša V., Krs M., Krsová M. & Pruner P., 1996b: Magnetostratigraphic and micropalaeontological investigations along the Jurassic/Cretaceous boundary strata, Brodno near Žilina (Western Slovakia). *Geol. Carpathica,* 47, 3, 135–151.

Jelínek V., 1966: A high sensitivity spinner magnetometer. *Stud. Geophys. Geod.,* 10, 58–78.

Jelínek V., 1973: Precision A.C. bridge set for measuring magnetic susceptibility and its anisotropy. *Stud. Geophys. Geod.,* 17, 36–48.

Jelínek V., 1977: The statistical theory of measuring anisotropy of magnetic susceptibility of rocks and its application. *Geofyzika,* Brno, 1–92.

Kate W. G. ten & Sprenger A., 1989: On the periodicity in a calcilutite-marl succession (SE Spain). *Cretaceous Research*, 10, 1–31.

Kirschvink J.L., 1980: The least-squares line and plane and the analysis of palaeomagnetic data. *Geophys. J. Roy. astron. Soc. (Oxford),* 62, 699–718.

Lowrie W. & Channell J.E.T., 1983: Magnetostratigraphy of the Jurassic-Cretaceous boundary in the Maiolica limestone (Umbria, Italy). *Geology,* 12, 44–47.

Márton E., 1986: The problems of correlation between magnetozones and calpionellid zones in Late Jurassic – Early Cretaceous section. *Acta Geol. Hung.,* 29 (1–2), 125–131.

Ogg J.G., Hasenyager R.W., Wimbledon W.A., Channell J.E.T. & Bralower T.J., 1991: Magnetostratigraphy of the Jurassic-Cretaceous boundary interval — Tethyan and English faunal realms. *Cretaceous Research*, 12, 455–482.

Ogg J.G., Steiner M.B., Company M. & Tavera J.M., 1988: Magnetostratigraphy across the Berriasian – Valanginian stage boundary (Early Cretaceous), at Cehegin (Murcia Province, southern Spain). *Earth Planet. Sci. Lett.,* 87, 205–215.

Ogg J.G., Steiner M.B., Oloriz F. & Tavera J.M., 1984: Jurassic magnetostratigraphy, 1. Kimmeridgian-Tithonian of Sierra Gorda and Carcabuey, southern Spain. *Earth Planet. Sci. Lett.,* 71, 147–162.

Parés J.M. & Roca E., 1996: The significance of tectonic-related Tertiary remagnetization along the margins of the Valencia through. *J. Geodynamics*, 22, 207–227.

Příhoda K., Krs M., Pešina B. & Bláha J., 1989: MAVACS — a new system of creating a non-magnetic environment for palaeomagnetic studies. *Cuad. Geol. Ibér.,* 12, 1988-1989, 223–250.

Sprenger A. & Kate W. G. ten, 1992: Orbital forcing of calcilutite-marl cycles in southeast Spain and an estimate for the duration of the Berriasian stage. *Geol. Soc. Amer. Bull.,* 105, 807–818.

Veen G. E.W. van., 1969: Geological investigations in the region west of Caravaca, south-eastern Spain. *Ph.D. thesis*, University of Amsterdam, 1–143.

Villalaín J.J., Osete M.L., Vegas R., García-Duenas V. & Heller F., 1996: The Neogene remagnetization in the western Betics: a brief comment on the reliability of palaeomagnetic directions. In: Morris A. & Tarling D.H. (Eds.): *Palaeomagnetism and Tectonics of the Mediterranean Region. Spec. Publ. (Geol. Soc. London),* 105, 33–41.

Zeiss A., 1986: Comments on tentative correlation chart for the most important marine provinces at the Jurassic/Cretaceous boundary. *Acta Geol. Hung.,* 29, 27–30.